SUPPLEMENTAL FIGURES:

Figure S1

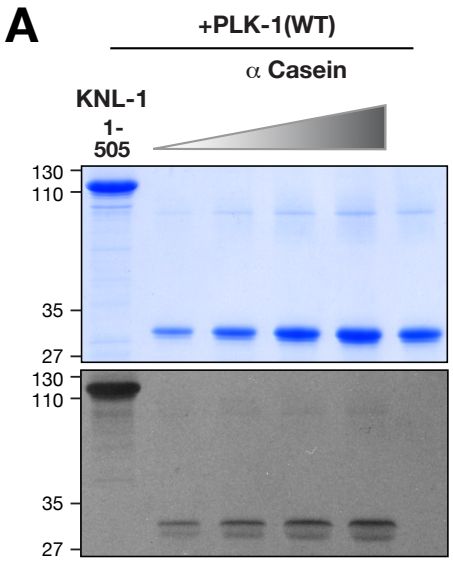
A
+PLK-1(WT)
α Casein
KNL-1
1-
505
130
110
35
27
130
110
35
27

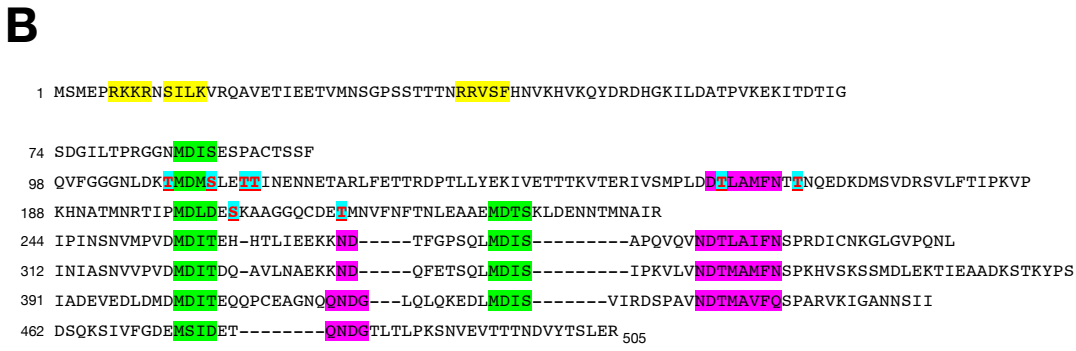
B
1 MSMEPRKKRNSILKVRQAVETIEETVMNSGPSSTTTNRRVSFHNVKHVKQYDRDHGKILDATPVKEKITDTIG
74 SDGILTPRGGNMDISESPACTSSF
98 QVFGGGNLDKTMDMSLETTINENNNETARLFETTRDPTLLYEKIVETTTKVTERIVSMPLDDTLAMFNTTNQEDKDMSVDRSVLFTIPKVP
188 KHNATMNRTIPMDLDESKAAGGQCDETMNVFNFTNLEAAEMDTSKLDENNTMNAIR
244 IPINSNVMPVDMDITEH-HTLIEEKKND-----TFGPSQLMDIS---------APQVQVNDTLAIFNSPRDICNKGLGVPQNL
312 INIASNVVPVDMDITDQ-AVLNAEKKND-----QFETSQLMDIS---------IPKVLVNDTMAMFNSPKHVSKSSMDLEKTIEAADKSTKYPS
391 IADEVEDLDMDMDITEQQPCEAGNQQNDG---LQLQKEDLMDIS-------VIRDSPAVNDTMAVFQSPARVKIGANNSII
462 DSQKSIVFGDEMSIDET--------QNDGTLTLPKSNVEVTTTNDVYTSLER 505

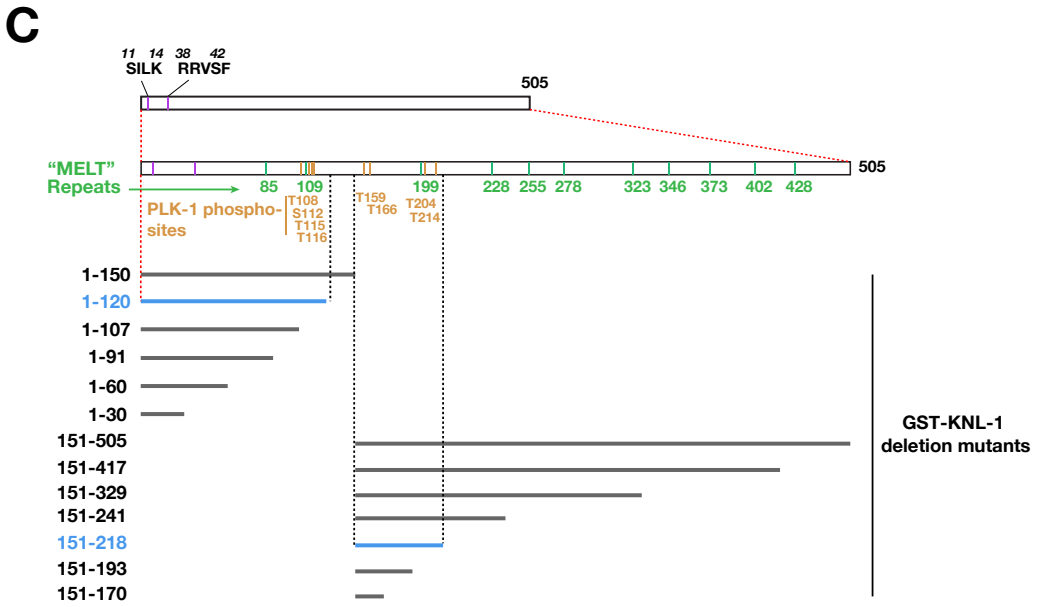
C
11 14 38 42
SILK RRVSF
505
"MELT" Repeats
505
85 109 199 228 255 278 323 346 373 402 428
PLK-1 phospho-sites
T108 S112 T115 T116
T159 T166
T204 T214
1-150
1-120
1-107
1-91
1-60
1-30
151-505
151-417
151-329
151-241
151-218
151-193
151-170
GST-KNL-1 deletion mutants

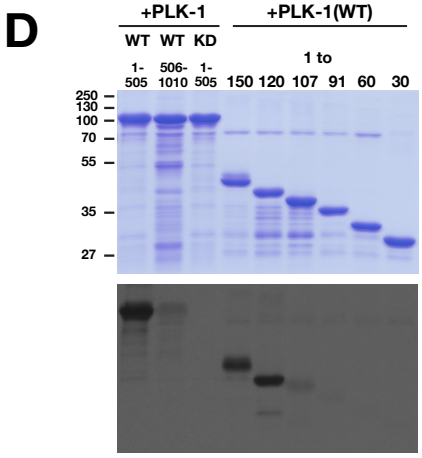
D
+PLK-1
+PLK-1(WT)
WT WT KD
1-505 506-1010 1-505
1 to
150 120 107 91 60 30
250
130
100
70
55
35
27

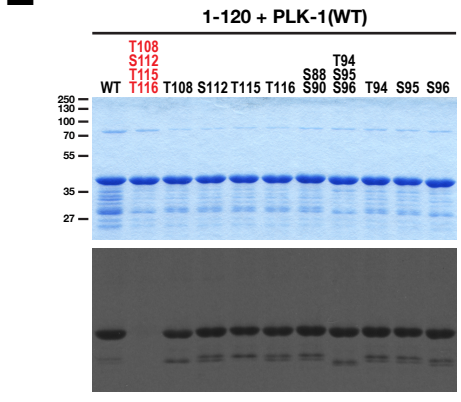
E
1-120 + PLK-1(WT)
T108 S112 T115
T94 S95
S88 S90
WT T116 T108 S112 T115 T116 T94 S95 S96
250
130
100
70
55
35
27

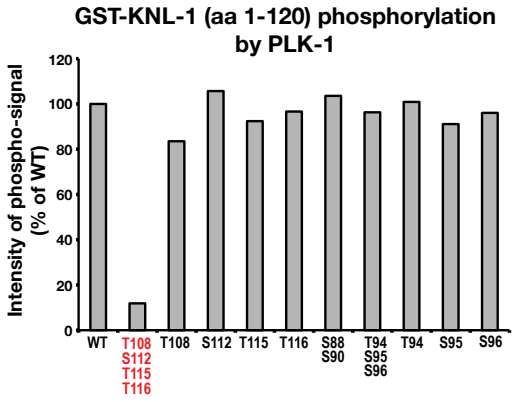
GST-KNL-1 (aa 1-120) phosphorylation by PLK-1
Intensity of phospho-signal (% of WT)
120
100
80
60
40
20
0
WT
T108 S112 T115 T116
T108
S112
T115
S88 S90
T94 S95 S96
T94
S95
S96

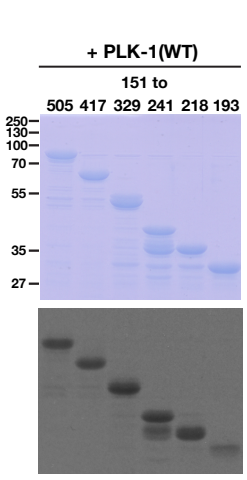
F
+ PLK-1(WT)
151 to
505 417 329 241 218 193
250
130
100
70
55
35
27

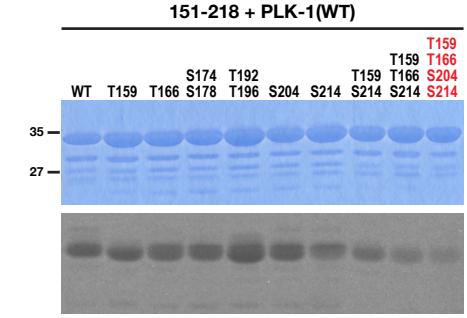
G
151-218 + PLK-1(WT)
T159 T166 S204 S214
T159 T166 S214
T159 S214
S174 S178
T192 T196
S204
S214
WT T159 T166
35
27

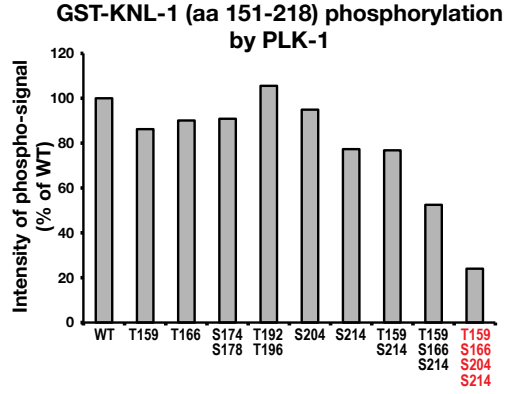
GST-KNL-1 (aa 151-218) phosphorylation by PLK-1
Intensity of phospho-signal (% of WT)
120
100
80
60
40
20
0
WT
T159
T166
S174 S178
T192 T196
S204
S214
T159 S214
T159 S166 S214
T159 S166 S204 S214

Figure S2

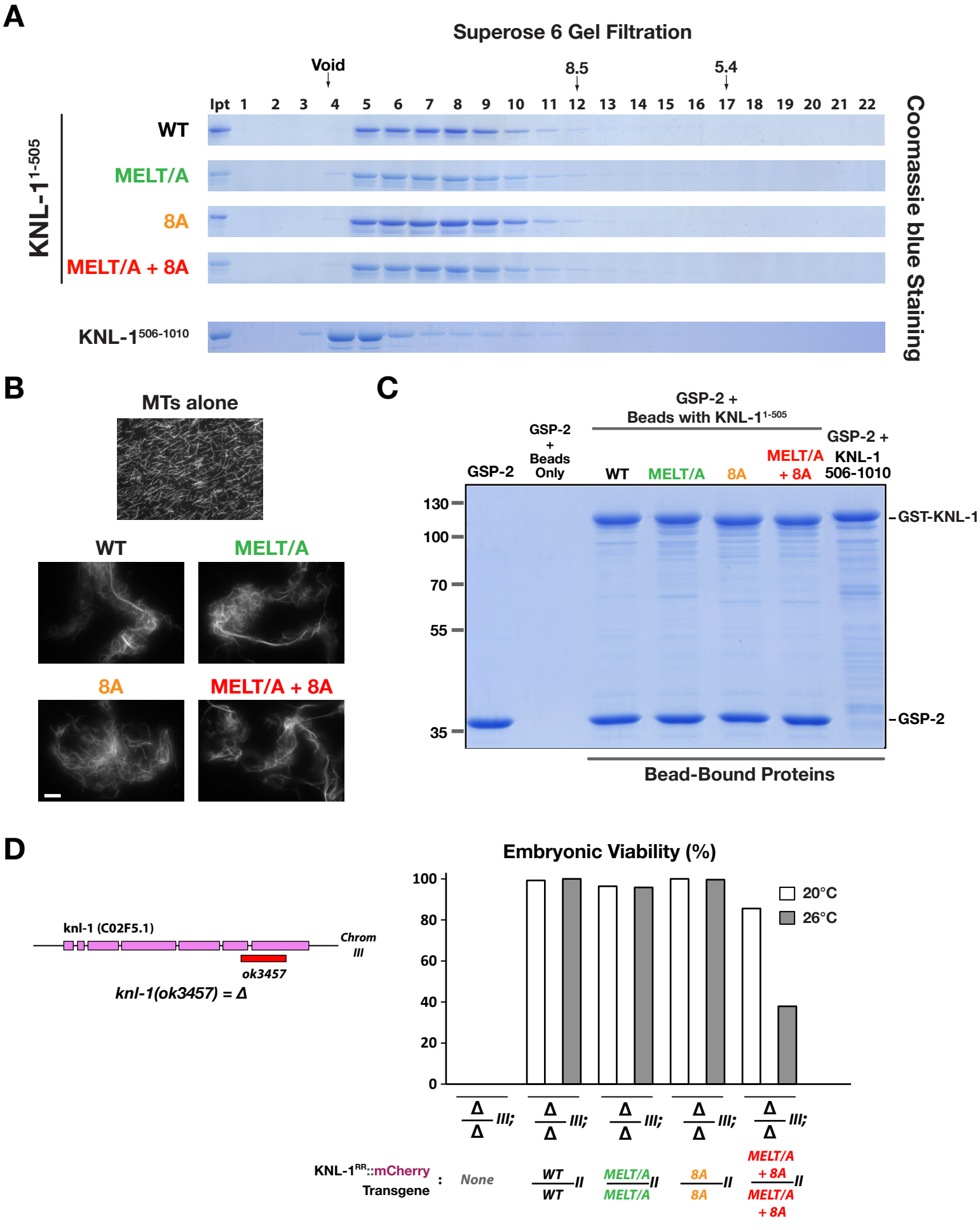
A
Superose 6 Gel Filtration
Void
8.5
5.4
lpt 1 2 3 4 5 6 7 8 9 10 11 12 13 14 15 16 17 18 19 20 21 22
KNL-1 1-505
WT
MELT/A
8A
MELT/A + 8A
KNL-1 506-1010
Coomassie blue Staining
B
MTs alone
WT
MELT/A
8A
MELT/A + 8A
C
GSP-2 + Beads with KNL-1 1-505
GSP-2
GSP-2 + Beads Only
WT
MELT/A
8A
MELT/A + 8A
GSP-2 + KNL-1 506-1010
130
100
70
55
35
GST-KNL-1
GSP-2
Bead-Bound Proteins
D
knl-1 (C02F5.1)
Chrom III
ok3457
knl-1(ok3457) = Δ
Embryonic Viability (%)
100
80
60
40
20
0
20°C
26°C
Δ/Δ III;
KNL-1 RR ::mCherry Transgene :
None
WT/WT II
MELT/A MELT/A II
8A/8A II
MELT/A + 8A / MELT/A + 8A II

Figure S3

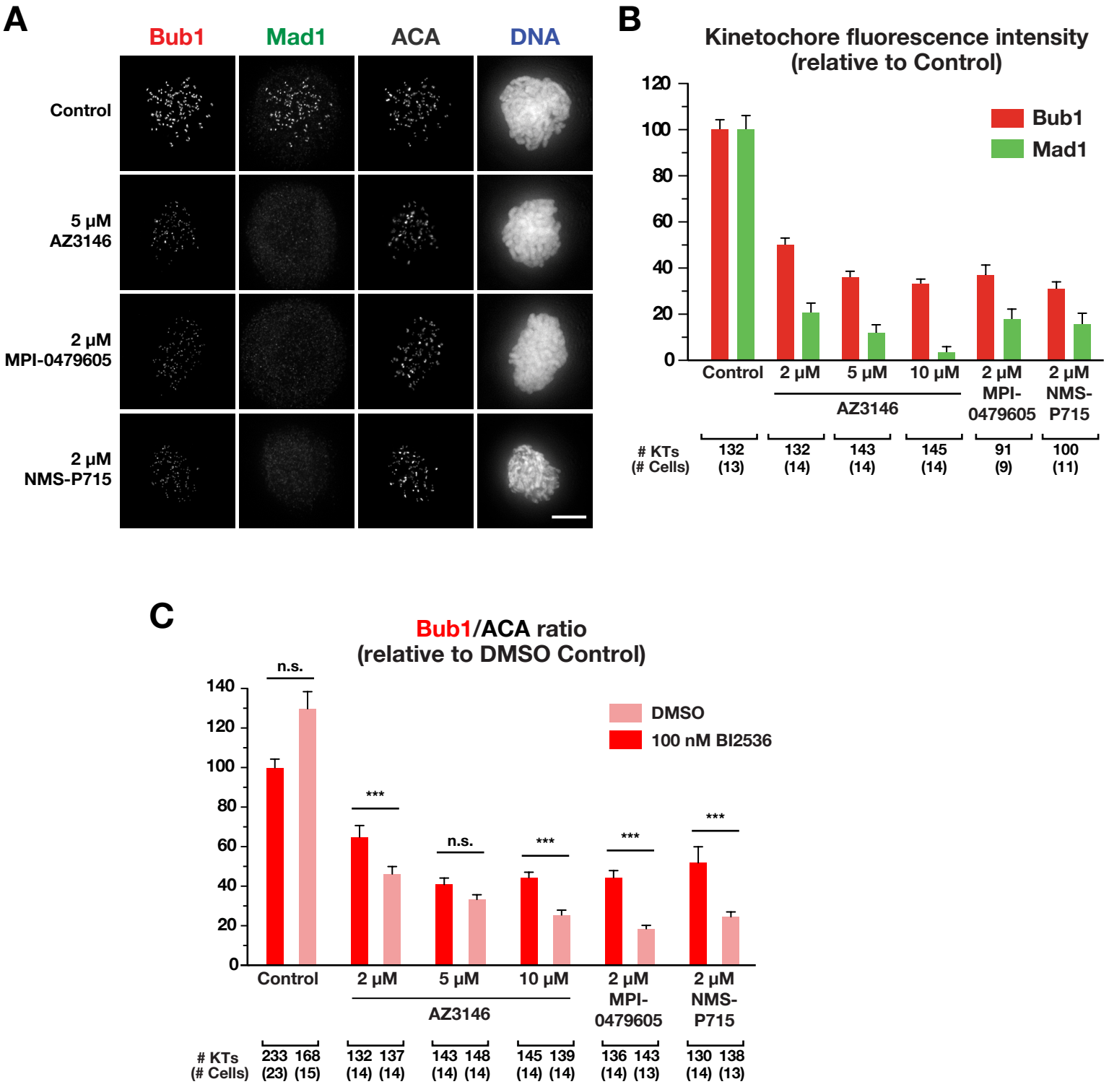
A
Bub1
Mad1
ACA
DNA
Control
5 μM AZ3146
2 μM MPI-0479605
2 μM NMS-P715
B
Kinetochore fluorescence intensity (relative to Control)
Bub1
Mad1
120
100
80
60
40
20
0
Control
2 μM
5 μM
10 μM
AZ3146
2 μM MPI-0479605
2 μM NMS-P715
KTs (# Cells)
132 (13)
132 (14)
143 (14)
145 (14)
91 (9)
100 (11)
C
Bub1/ACA ratio (relative to DMSO Control)
DMSO
100 nM BI2536
n.s.
***
n.s.
***
***
***
140
120
100
80
60
40
20
0
Control
2 μM
5 μM
10 μM
AZ3146
2 μM MPI-0479605
2 μM NMS-P715
KTs (# Cells)
233 168 (23) (15)
132 137 (14) (14)
143 148 (14) (14)
145 139 (14) (14)
136 143 (14) (13)
130 138 (14) (13)

Figure S4

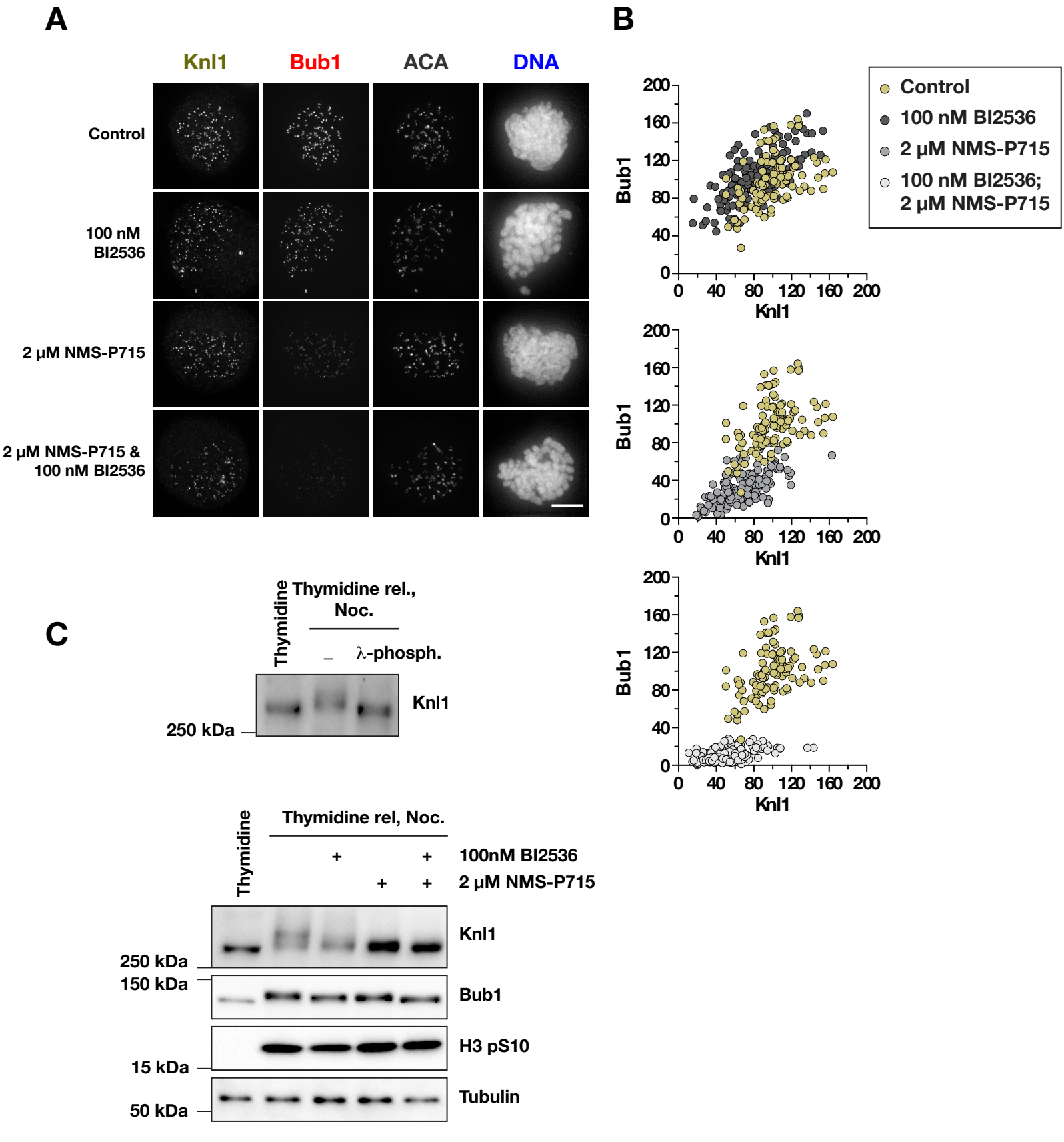
A
Knl1
Bub1
ACA
DNA
Control
100 nM BI2536
2 µM NMS-P715
2 µM NMS-P715 & 100 nM BI2536
B
Control
100 nM BI2536
2 µM NMS-P715
100 nM BI2536; 2 µM NMS-P715
Bub1
Knl1
0
40
80
120
160
200
C
Thymidine
Thymidine rel., Noc.
λ-phosph.
Knl1
250 kDa
Thymidine rel, Noc.
100nM BI2536
2 µM NMS-P715
Knl1
Bub1
H3 pS10
Tubulin
250 kDa
150 kDa
15 kDa
50 kDa

SUPPLEMENTAL FIGURE LEGENDS

Figure S1, related to Fig. 1. Analysis of KNL-1$^{1-505}$ phosphorylation by PLK-1.

(A) PLK-1 kinase assays employing GST-KNL-1$^{1-505}$ and α–casein as substrates. PLK-1 was ~7-fold more active towards KNL-1$^{1-505}$ than and equimolar concentration of α-casein.

(B) Alignment of KNL-1 primary sequence repeats. In the repeats, the MELTs are in green followed by ND sequences in purple. The basic patch necessary for microtubule binding (RKKR) and the PP1 binding site (SILK/RRVSF) are in yellow. Sites identified in this study as being phosphorylated by PLK-1 are in underlined red text that is highlighted in cyan.

(C) Thirteen deletion mutants and nineteen mutants harboring different combinations of single alanine mutations were engineered in order to identify the amino-acids phosphorylated by PLK-1 *in vitro*. MELT repeats are highlighted in green. Phospho-sites identified are highlighted in orange.

(D) Analysis of KNL-1$^{1-150}$ and sub-fragment phosphorylation by PLK-1. There was no decrease in phosphorylation of the 1-120 fragment compared to the 1-150 mutant, but phosphorylation was reduced to ~17 % for the 1-107 mutant, indicating that the major phosphorylation sites in aa 1-150 of KNL-1 were located in aa 107-120.

(E) Analysis of PLK-1 phosphorylation of alanine mutants of KNL-1$^{1-150}$. Coomassie Blue staining and autoradiography with indicated single alanine mutant KNL-1$^{1-150}$ substrates (*left*). Phospho-signal intensity was quantified and normalized relative to the control (WT) (*right*). In this region, 4 sites (T108, S112, T115, T116) fit the PLK-1 consensus. We performed site directed mutagenesis on these sites and on other adjacent ones (S88, S90, T94, S95, S96) to determine if they are phosphorylated by PLK-1. The T108, S112, T115 and T116 sites mutated individually into alanine did not exhibit significant decrease in phosphorylation compared to the WT but when combined (4A mutant), 88% of the signal

was lost. In contrast, mutations in other residues did not affect KNL-1^{1-120} phosphorylation levels, indicating that the T108, S112, T115 and T116 amino acids are the major sites phosphorylated by PLK-1 in this region.

(F-G) Analysis of KNL-$1^{151-505}$ and sub-fragment phosphorylation by PLK-1. We adopted a deletion and site directed mutagenesis approach, similar to that employed for KNL-1^{1-150}. to determine target sites in the 151-505 region. The major phosphorylation sites were located in aa 151-218 (*F*). Analysis of alanine mutants revealed that T159, T166, S204 and S214 are the major sites in this region. In contrast, mutation of S174 + S178 or T179 + T196 did not affect KNL-1 phosphorylation.

Figure S2, related to Fig. 1 and Fig. 3. ***Mutation of MELT repeats and/or mapped PLK-1 target sites in KNL-1^{1-505} does not affect oligomerization status, microtubule binding, or ability to dock PP1; MELT/A+8A compromises embryo viability.***

(A) Analysis of recombinant KNL-1^{1-505} proteins by gel-filtration. All 4 KNL-1^{1-505} proteins (WT, MELT/A, 8A, MELT/A+8A) exhibited a similar elution profile by gel filtration, indicating that the introduced mutations do not alter oligomerization of KNL-1. KNL-$1^{506-1010}$ has a different profile than KNL-1^{1-505} suggesting that N- and C-terminal halves of the protein have different oligomerization status or different shapes. A Superose 6 column was used for gel filtration chromatography and fractions were analyzed by SDS-PAGE followed by Coomassie Blue staining.

(B) Microtubule bundling analysis of recombinant KNL-1^{1-505} proteins. 1 μM of GMPCPP-stabilized rhodamine microtubules were imaged either alone, or in the presence of indicated 2 μM KNL-1^{1-505} variants. Scale bar, 10 μm.

(C) Biochemical analysis of KNL-1 interaction with GSP-2. Indicated variants of GST-KNL-1 were immobilized on GST beads and incubated with GSP-2-6xhis. Beads were washed and bound proteins analyzed by SDS-PAGE.

(D) (*left panel*) Schematic representation of the deletion mutant *knl-1(ok3457)*. (*right panel*) Embryo viability of the *knl-1(ok3457)* deletion mutant in the presence of WT, MELT/A, 8A and MELT/A+8A KNL-1 variants. Embryo viability was monitored at 20°C or 26°C.

Figure S3, related to Fig. 4. ***Effect of Mps1 and Plk1 inhibition on Bub1 and Mad1 recruitment in HeLa cells.***

(A) Representative immunofluorescence images of mitotic HeLa cells treated with Mps1 inhibitors AZ3146, MPI-0479605, NMS-P715 and stained for Bub1 and Mad1.

(B) Quantification of Bub1 and Mad1 kinetochore intensities following treatment with different concentrations of the Mps1 inhibitors AZ3146, MPI-0479605, NMS-P715. Values are normalized to controls. Error bars represent the 95% confidence interval.

(C) Quantification of Bub1/ACA ratios for the indicated inhibitor treatments. Values are normalized to controls. Error bars represent the 95% confidence interval. ***: $p < 0.0001$

Figure S4, related to Fig. 4. ***Effect of Plk1 and Mps1 inhibition on Knl1 recruitment.***

(A) Representative immunofluorescence images of mitotic HeLa cells treated with BI2536, NMS-P715 or the combination of both and stained for Bub1 and Knl1. Bar, 5 μm.

(B) Scatter plot showing the relationship between Knl1 and Bub1 kinetochore intensities for the different treatments. Each point represents an individual kinetochore quantified for both Knl1 and Bub1.

(C) Immunoblot analysis of mitotic Knl1 phosphorylation, as monitored by the mobility shift that is eliminated by λ-phosphatase treatment, under the different drug treatments.

SUPPLEMENTAL TABLES

Table S1, related to Figure 4. *Mps1, Plk1 and Aurora B IC_{50} values for Mps1 inhibitors used in this study.*

Kinase	IC_{50} (μM)			
	AZ3146	**NMS-P715**	**MPI-0479605**	**Reversine**
Mps1	0.0048	0.0056	0.016	*0.0058*
Plk1	0.75	0.72	5.23	*1.18*
Aurora B	>10	>10	>10	*0.069*

Inhibitory potencies were determined by Reaction Biology Corporation (http://www.reactionbiology.com/) using high throughput Kinase HotSpot radiometric assays. ([ATP] = 10 μM, n = 4-6; Mps1 K_m(ATP) = 50 μM; Plk1 K_m(ATP) = 33 μM; Aurora B K_m(ATP) > 200 μM). AZ3146 (Tocris Bioscience), NMS-P715 (EMD Millipore), MPI-0479605 (Selleck Chemicals) and Reversine (Sigma-Aldrich) were tested. MPI-0479605 exhibits significant structural similarity to Reversine, but is more specific in that it lacks the potent, and potentially confounding, Aurora kinase inhibitory properties of Reversine (Santaguida et al., 2010).

Table S2, related to Figures 1-3. *C. elegans strains used in this study*

Strain #	Genotype
N2	*wild-type (ancestral N2 Bristol)*
TH32	*unc-119(ed3) III; ruIs32 [pAZ132; pie-1/GFP::his-58; unc-119(+)] III; ddIs6 [pie-1/GFP::tbg-1; unc-119(+)]V*
OD334/JES11	*unc-119(ed3) III; ltSi1 [pOD809/pJE110; Pknl-1::KNL-1reencoded::mCherry; cb-unc-119(+)]II*
JES154	*unc-119(ed3) III; ijpSi30 [pJE296; Pknl-1::KNL-1reencoded(MELT/A)::mCherry; cb-unc-119(+)]II*
JES156	*unc-119(ed3) III; ijpSi32 [pJE301; Pknl-1::KNL-1reencoded(8A)::mCherry; cb-unc-119(+)]II*
JES158	*unc-119(ed3) III; ijpSi34 [pJE312; Pknl-1::KNL-1reencoded(MELT/A+8A)::mCherry; cb-unc-119(+)]II*
OD373/JES16	*unc-119(ed3) III; ltSi9 [pOD831/pJE120; Pknl-1::KNL-1reencoded(RRASA)::mCherry; cb-unc-119(+)]II*
OD388/JES21	*unc-119(ed3) III; ltSi1 [pOD809/pJE110; Pknl-1::KNL-1reencoded::mCherry; cb-unc-119(+)]II; ruIs32 [pAZ132; pie-1/GFP::his-58; unc-119(+)] III; ddIs6 [pie-1/GFP::tbg-1; unc-119(+)]V*
JES160	*unc-119(ed3) III; ijpSi30 [pJE296; Pknl-1::KNL-1reencoded(MELT/A)::mCherry; cb-unc-119(+)]II; ruIs32 [pAZ132; pie-1/GFP::his-58; unc-119(+)] III; ddIs6 [pie-1/GFP::tbg-1; unc-119(+)]V*
JES162	*unc-119(ed3) III; ijpSi32 [pJE301; Pknl-1::KNL-1reencoded(8A)::mCherry; cb-unc-119(+)]II; ruIs32 [pAZ132; pie-1/GFP::his-58; unc-119(+)] III; ddIs6 [pie-1/GFP::tbg-1; unc-119(+)]V*
JES164	*unc-119(ed3) III; ijpSi34 [pJE312; Pknl-1::KNL-1reencoded(MELT/A+8A)::mCherry; cb-unc-119(+)]II; ruIs32 [pAZ132; pie-1/GFP::his-58; unc-119(+)] III; ddIs6 [pie-1/GFP::tbg-1; unc-119(+)]V*
JES170	*unc-119(ed3) III; ltSi1 [pOD809/pJE110; Pknl-1::KNL-1reencoded::mCherry; cb-unc-119(+)]II; ddIs68[bub-1::TY1::EGFP::3xFLAG(92C12)+unc-119(+)]*
JES161	*unc-119(ed3) III; ijpSi30 [pJE296; Pknl-1::KNL-1reencoded(MELT/A)::mCherry; cb-unc-119(+)]II; ddIs68[bub-1::TY1::EGFP::3xFLAG(92C12)+unc-119(+)]*
JES163	*unc-119(ed3) III; ijpSi32 [pJE301; Pknl-1::KNL-1reencoded(8A)::mCherry; cb-unc-119(+)]II; ddIs68[bub-1::TY1::EGFP::3xFLAG(92C12)+unc-119(+)]*
JES165	*unc-119(ed3) III; ijpSi34 [pJE312; Pknl-1::KNL-1reencoded(MELT/A+8A)::mCherry; cb-unc-119(+)]II; ddIs68[bub-1::TY1::EGFP::3xFLAG(92C12)+unc-119(+)]*
OD391/JES24	*unc-119(ed3) III; ltSi1 [pOD809/pJE110; Pknl-1::KNL-1reencoded::mCherry; cb-unc-119(+)]II;* ltIs52 *[*pOD379; pie-1/GFP::Y69A2AR.30; unc-119 *(+)]*
JES175	*unc-119(ed3) III; ijpSi30 [pJE296; Pknl-1::KNL-1reencoded(MELT/A)::mCherry; cb-unc-119(+)]II;* ltIs52 *[*pOD379; pie-1/GFP::Y69A2AR.30; unc-119 *(+)]*
JES176	*unc-119(ed3) III; ijpSi32 [pJE301; Pknl-1::KNL-1reencoded(8A)::mCherry; cb-unc-119(+)]II;* ltIs52 *[*pOD379; pie-1/GFP::Y69A2AR.30; unc-119 *(+)]*
JES177	*unc-119(ed3) III; ijpSi34 [pJE312; Pknl-1::KNL-1reencoded(MELT/A+8A)::mCherry; cb-unc-119(+)]II;* ltIs52 *[*pOD379; pie-1/GFP::Y69A2AR.30; unc-119 *(+)]*
VC2787	*(+/mT1 II; knl-1(ok3457)/mT1[dpy-10(e128)] III)* - Source strain for KNL-1Δ
EG4322	*unc-119(ed3) III; ttTi5605 II* - Source for KNL-1^{RR}::mCherry transgenic strains

Table S3, related to Figures 1-3. *dsRNAs used in this study*

Gene #	Name	Conc mg/ml	Oligo #1	Oligo #2	Template
C02F5.1	knl-1	3.1	AATTAACCCTCACTAAAGG aatctcgaatcaccgaaatgtc	TAATACGACTCACTATAG Gttcacaaacttggaagccgctg	cDNA
F59E12.2	zyg-1	2.6	AATTAACCCTCACTAAAGGt ggacggaaattcaaacgat	TAATACGACTCACTATAG Gaacgaaattcccttgagctg	cDNA
Y69A2AR.30	mdf-2	2.2	TAATACGACTCACTATAGG gagaccacacggatgtaaagacaca aaacg	TAATACGACTCACTATAG Ggagaccacgtgaactgacgtcga gaatgag	cDNA

SUPPLEMENTAL EXPERIMENTAL PROCEDURES

Protein Purification and Pulldown Assays

KNL-1 and GSP-2 open reading frames were amplified from N2 cDNA and cloned into pGEX6P-1 and pET21A, respectively. Expression in Rosetta (DE3) pLysS *E. coli* was induced with 0.3 mM IPTG for 4 hr at 20°C and GST and 6xHis purifications performed using standard procedures. KNL-1 proteins were purified into TD buffer (40 mM Tris [pH 7.5], 250 mM NaCl, 0.5 mM EDTA, 5 mM BME) and eluted with 40 mM glutathione. For gel filtration and microtubule bundling assays, KNL-1 proteins bound to GST beads were first eluted by Prescission protease digestion of the cleavage site present between the GST tag and the KNL-1 N-terminus. The cleaved eluted proteins were exchanged into SP buffer (30 mM MOPS [pH 7.0], 50 mM NaCl, 0.5 mM EDTA, 2 mM BME), bound to HiTrap SP sepharose (GE Bio-sciences), eluted with a gradient from 50 to 500 mM NaCl, and dialyzed to reduce the salt concentration to 100 mM NaCl, or exchanged into BRB80 (80 mM PIPES [pH 6.8], 1 mM EGTA, 1 mM $MgCl_2$) + 80 mM KCl. For GSP-2, imidazole-eluted protein was exchanged into 30 mM HEPES [pH 7.0], 50 mM NaCl, 0.1 mM EDTA, 2 mM BME, bound to HiTrap SP sepharose and eluted with a gradient from 50 to 500 mM NaCl, followed by dialysis to 100 mM NaCl.

For pulldown assays, 3 micrograms KNL-$1^{1\text{-}505}$ or KNL-$1^{506\text{-}1010}$ were immobilized on 20 µl GST agarose resin (Qiagen) for 1 h at 4°C. The resin was then washed three times (Wash buffer: 50 mM HEPES [pH 7.5], 100 mM NaCl, 2 mM $MnCl_2$, 0.1 mM EDTA, 0.1% Tween-20, 10% Glycerol, 5 mM BME) and incubated 1 h at room temperature with 10 micrograms purified 6his-GSP-2 protein in 60µl volume. The resin was then washed three times, eluted with sample buffer, and analyzed by SDS-PAGE.

Plk1 open reading frame was amplified from N2 cDNA and cloned into pFastBacHTb vector. Plk1 kinase dead (KD) version was obtained by direct mutagenesis of the N166 amino acid into alanine. Plk1 WT or KD proteins were expressed into SF9 insect cells and 6his purifications were performed using standard procedures. Cells were lysed into 50mM Hepes [pH 7.4], 200mM NaCl, 2mM $MgCl_2$ and 15% glycerol, eluted in the same buffer supplemented by 250mM imidazole followed by dialysis to 100mM NaCl.

BUB-1(1-494) and BUB-3 FL were cloned into pGADT7 plasmids and expressed in reticulocyte lysates in the presence of [35S]-Methionine using the TNT Quick Coupled Transcription/Translation system (Promega). Binding assays were performed by incubating GST-KNL-1^{1-505} phosphorylated or not by PLK-1 in the presence of Adenosine 5′-[γ-thio]triphosphate (ATP-γ-S), with BUB-1^{1-494} and BUB-3 expressed in reticulocyte lysates for 1 hour at room temperature. Beads were washed and eluted with 40mM glutathione. Eluted proteins were analysed by Coomassie staining and autoradiography.

Kinase assays

Dephosphorylated α-casein (Sigma #8032) was used at concentrations between 5.6 μM (0.13 g/l) and 18.5 μM (0.425 g/l). Quantification of phosphorylation was performed with the gel analysis tools in Image J. A rectangle was drawn around the bands of interest and integrated pixel intensity was measured. The rectangle was displaced up to define the background intensity and the difference in integrated intensity between the original rectangle and the upper rectangle was used to measure band intensity.

Microtubule Bundling Assay

For microtubule bundling assays, 1 μM taxol stabilized Atto 488 (Atto-Tec GmbH) microtubules were mixed with 1 μM KNL-1^{1-505} variants or control buffer. After 5 min incubation, the mixture was imaged using a 60X, 1.4NA Planapo objective.

Worm Strains, RNA Interference

C. elegans strains used in this study (**Table S2**) were maintained at 20°C. Engineered transgenes were cloned into pCFJ151 (Espeut et al., 2012; Frokjaer-Jensen et al., 2008) and injected into strain EG4322 to obtain stable single-copy integrants. Integration of transgenes was confirmed by PCR and homogeneous KNL-1::mCherry fluorescence in all progeny. Transgenic strains were then crossed into various marker strains using standard genetic procedures prior to analysis.

For RNAi, L4 worms were injected with double-stranded RNAs (**Table S3**) and incubated for 38-43h at 20°C. For double depletions, dsRNAs were mixed to obtain equal concentrations of ≥0.75 mg/mL for each dsRNA. To test the temperature sensitivity of the KNL-1 mutant strains, the worms were shifted from 20°C to 26°C 2 hours before imaging, which was performed at 26°C.

Immunofluorescence in human cells

For drug treatment of HeLa cells, nocodazole was used at 3.3 μM, MG132 at 10 μM and BI2536 at 100 nM. AZ3146 (Tocris Bioscience), NMS-P715 (EMD Millipore) and MPI-0479605 (Selleck Chemicals) were used at 2 μM unless otherwise specified.

For all human cell experiments, we used a double thymidine synchronization protocol, followed by treatment with Mps1 and/or Plk1 inhibitors, as well as nocodazole,

prior to mitotic entry (see schematic in **Fig. 4A**). The reason for this is because attachment of kinetochores to microtubules removes Mad1, and partially Bub1 (Jablonski et al., 1998; Taylor et al., 2001), which introduces variation in kinetochore fluorescence intensity measurements based on attachment status. In addition, inhibition of Mps1 has been reported to affect Mad1 localization only when added before mitotic entry, but not once cells are already in mitosis (Hewitt et al., 2010).

For immunofluorescence, cells were washed with PBS, fixed in 1% formaldehyde for 5 minutes, permeabilized in PBS containing 0.1% Triton X-100 (PBS-T) and blocked with PBS containing either 12.5 mM glycine pH 8.5 or 3% BSA for Knl1 pT875 staining. For visualization of kinetochore proteins, cells were incubated with the following antibodies: sheep anti-Bub1 (1:4000; a gift from Stephen Taylor, University of Manchester, UK), mouse anti-Mad1 clone 9B10 (1:500; Millipore), rabbit anti-Knl1 (1:1000, (Cheeseman et al., 2008), rabbit anti-Knl1 phospho-T875 (Yamagishi et al., 2012) and ACA (1:250; Antibodies Incorporated) in blocking solution. After washes in PBS-T, cells were incubated with secondary antibodies conjugated with Cy2, Cy3 or Cy5 fluorophores (Jackson Immunoresearch). DNA was visualized with 10 µg/ml Hoescht in PBS. Coverslips were mounted in 0.5% p-phenylenediamine and 20 mM Tris-Cl, pH 8.8, in 90% glycerol.

Images were recorded on a Deltavision microscope at 1X1 binning with a 100X NA 1.3 U-planApo objective. Z-stacks (0.5 µm sections) were deconvoluted using softWorRx (Applied Precision) and maximum intensity projections were imported into Adobe Photoshop for further processing.

Quantification of signal intensities* C. elegans *embryos and human cell immunofluorescence experiments

Analysis of *C. elegans* embryo images was performed with Image J software. Quantification of BUB-1 kinetochore localization during metaphase of one-cell embryos and MAD-2^{MDF-2} on monopolar two-cell embryos was performed on maximum intensity projections. A rectangle was drawn around the kinetochore signal, and integrated pixel intensity was measured. The rectangle was expanded by 4 pixels on all sides, and the difference in integrated intensity between the expanded rectangle and the original rectangle was used to define the background intensity per pixel (**Fig. 2C**). Integrated kinetochore fluorescence was then calculated for the original rectangle after background subtraction.

For quantification of kinetochore intensities in human cells, projections were analyzed with Metamorph software, as described (Hoffman et al., 2001). Briefly, 13 X 13 and 18 X 18 pixel squares were drawn around single kinetochores in the ACA channel and then transferred to other channels. Integrated pixel intensities for each square were measured and the difference between the two squares was used to estimate background intensity. Integrated kinetochore intensities were then calculated from the 13 X 13 pixel square after background subtraction. p-values were estimated using a nonparametric ANOVA (Kruskal-Wallis) test followed by a Dunn's post-test.

Immunoblotting of HeLa cell lysates

HeLa cells were synchronized and treated as described in **Fig. 4A** and lysed in 1.5X Laemmli sample buffer. Proteins were separated by SDS-PAGE using either 13% polyacrylamide gels or NuPAGE 3-8% Tris-Acetate gels for Knl1 (Life Technologies), transferred to a nitrocellulose membrane and probed using the following antibodies: rabbit anti-Knl1 (Bethyl Laboratories), sheep anti-Bub1 (Taylor et al., 2001), rabbit anti-Histone H3

pSer10 (Sigma) and mouse anti-tubulin (DM1α, Sigma). After incubation with HRP-conjugated secondary antibodies, membranes were developed using Enhanced Chemiluminescence and imaged using a ChemiDoc MP imaging system (BioRad).

For λ-phosphatase treatment, soluble lysates were incubated with 400 units of λ-phosphatase (New England Biolabs) in 1X λ-phosphatase buffer, 1mM $MnCl_2$ and 0.1% triton X-100, for 15 minutes at 30°C, and then processed for immunoblotting as described above.

SUPPLEMENTAL REFERENCES

Cheeseman, I.M., Hori, T., Fukagawa, T., and Desai, A. (2008). KNL1 and the CENP-H/I/K complex coordinately direct kinetochore assembly in vertebrates. Mol Biol Cell *19*, 587-594.

Frokjaer-Jensen, C., Davis, M.W., Hopkins, C.E., Newman, B.J., Thummel, J.M., Olesen, S.P., Grunnet, M., and Jorgensen, E.M. (2008). Single-copy insertion of transgenes in Caenorhabditis elegans. Nat Genet *40*, 1375-1383.

Jablonski, S.A., Chan, G.K., Cooke, C.A., Earnshaw, W.C., and Yen, T.J. (1998). The hBUB1 and hBUBR1 kinases sequentially assemble onto kinetochores during prophase with hBUBR1 concentrating at the kinetochore plates in mitosis. Chromosoma *107*, 386-396.

Taylor, S.S., Hussein, D., Wang, Y., Elderkin, S., and Morrow, C.J. (2001). Kinetochore localisation and phosphorylation of the mitotic checkpoint components Bub1 and BubR1 are differentially regulated by spindle events in human cells. J Cell Sci *114*, 4385-4395.